C. R. Mecanique 342 (2014) 532–538

Contents lists available at ScienceDirect

Comptes Rendus Mecanique

www.sciencedirect.com

# Experimental study of the response of a flexible plate to a harmonic forcing in a flow

## *Étude expérimentale de la réponse d'une plaque flexible à un forçage harmonique dans un écoulement*

Florine Paraz, Christophe Eloy, Lionel Schouveiler *

*Aix–Marseille Université, CNRS, Centrale Marseille, IRPHE UMR 7342, 13384 Marseille cedex 13, France*

ARTICLE INFO

*Article history:*
Received 14 April 2014
Accepted 10 June 2014
Available online 16 July 2014

*Keywords:*
Fluid–structure interaction
Flexible plate
Harmonic forcing
Resonance
Non-linearity
Propulsion

*Mots-clés :*
Interaction fluide–structure
Plaque flexible
Forçage harmonique
Résonance
Non-linéarité
Propulsion

ABSTRACT

Most aquatic animals propel themselves by flapping flexible appendages. To gain insight into the effect of flexibility on the swimming performance, we have studied experimentally an idealized system. It consists of a flexible plate whose leading edge is forced into a harmonic heave motion, and which is immersed in a uniform flow. As the forcing frequency is gradually increased, resonance peaks are evidenced on the plate's response. In addition to the forcing frequency, the Reynolds number, the plate rigidity and the forcing amplitude have also been varied. In the range of parameters studied, the main effect on the resonance is due to the forcing amplitude, which reveals that non-linearities are essential in this problem.



RÉSUMÉ

La plupart des animaux aquatiques se propulsent grâce au battement d'appendices flexibles. Afin d'avoir une meilleure compréhension de l'effet de la flexibilité sur la performance de la nage, nous avons étudié expérimentalement un système idéalisé. Il consiste en une plaque flexible, immergée dans un écoulement uniforme, dont le bord d'attaque est forcé en un mouvement harmonique transverse à l'écoulement. En augmentant graduellement la fréquence de forçage, des pics de résonance ont été mis en évidence. Outre la fréquence de forçage, on a également fait varier le nombre de Reynolds, la rigidité de la plaque et l'amplitude du forçage. Dans le domaine de paramètres étudié, le principal effet sur la résonance est dû à l'amplitude du forçage, ce qui révèle que les non-linéarités sont essentielles dans ce problème.



* Corresponding author.
*E-mail addresses:* florine.paraz@irphe.univ-mrs.fr (F. Paraz), christophe.eloy@irphe.univ-mrs.fr (C. Eloy), lionel.schouveiler@irphe.univ-mrs.fr (L. Schouveiler).

http://dx.doi.org/10.1016/j.crme.2014.06.004
1631-0721/

## 1. Introduction

Animal swimming has attracted a lot of attention from hydrodynamicists in the last decades. This interest was partly motivated by the design of bioinspired aquatic propulsion devices. Numerous reviews can be found on the different aquatic propulsion modes, such as the monographs of Lighthill [1] and Childress [2] or the articles of Lighthill [3], Sfakiotakis et al. [4] and Triantafyllou et al. [5]. Propulsion using flapping appendages is common for large aquatic animals and, in particular, most of the fast swimmers such as sharks, tuna and dolphins flap their caudal fins to propel themselves. An observation of these appendages shows that they are generally flexible along the chord. It has often been argued (e.g. [6] and [7]), that this flexibility enhances the swimming performance. However, the origin of this performance enhancement has proved elusive so far.

Inspired by this caudal-fin swimming mode, different studies have been carried out to quantify the propulsion efficiency of a flapping foil. Propulsion by rigid foils has been first studied theoretically by Lighthill [8] and Wu [9]. It has also been the object of experiments by Triantafyllou et al. [10], Anderson et al. [11], Schouveiler et al. [12], and Buchholz and Smits [13], among others. These experimental studies have all reported that propulsion performance is maximized for a flapping frequency $f$ corresponding to a Strouhal number $St \approx 0.3$, where $St = 2fA_{TE}/U$, with $A_{TE}$ the amplitude of the trailing edge motion and $U$ the swimming speed. The same value of $St \approx 0.3$ can be observed in nature for swimmers with moderate aspect ratios (cetaceans, sharks, salmons, trouts and scombrids) as seen in the data recently compiled in [14].

The numerical simulations of Katz and Weihs [15] have shown that, using a flapping foil flexible along its chord rather than a rigid one, yields an increase of the propulsive efficiency. In this case, because of the foil flexibility, its natural structural frequencies are introduced in the system, in addition to the flapping frequency. These structural frequencies depend not only on the geometry and the material of the foil but also on the surrounding flow because of added-mass effects. Two-dimensional numerical simulations of Alben [16] and Michelin and Llewellyn Smith [17] have later revealed peaks in the amplitude of the plate response, when the flapping and structural frequencies are resonant. They showed that efficiency can be maximized at these resonance peaks.

Gain in propulsive performance through the chordwise flexibility has been confirmed by the experimental works of Prempraneerach et al. [18], Heathcote and Gursul [19], or Marais et al. [20]. Moreover, Dewey et al. [21] for a pitching flexible plate, Alben et al. [22] and Quinn et al. [23] for a heaving flexible plate have clearly evidenced the phenomenon of resonance experimentally, as the forcing frequency is varied, and considered its link with propulsive performance, but none of these studies has considered the effect of changing the forcing amplitude.

In this study, to have a better understanding of the dynamics of a flexible fin, we have examined the response of an elastic plate immersed in a uniform flow and forced into a harmonic heave motion at its leading edge. The objective has been to quantify the influence of the different experimental parameters: the amplitude and frequency of forcing, the flow velocity, and the plate bending rigidity. This problem involves complex fluid–structure interactions since the flow load deforms the plate, whose motion in turn affects the flow. We believe that the full complexity of these interactions can only be addressed with experimental studies because, at the present time, accurate numerical simulations are limited to moderate Reynolds numbers and theoretical models usually assume linear problems, i.e. small-amplitude propulsion.

This paper is organized as follows: first the experimental set-up and methods are presented. Then the response of flexible plates to harmonic heave forcing is analyzed and effects of the different experimental parameters are discussed. Finally, some conclusions are drawn and discussed in the context of swimming.

## 2. Experimental set-up

Experiments have been conducted with the set-up schematically illustrated in Fig. 1(a). It consists of a horizontal flexible plate molded out of polysiloxane with a rounded leading edge and a tapered trailing edge (Fig. 1(b)). The plates used have a thickness $e = 0.004$ m, span $s = 0.12$ m, and chord $c = 0.12$ m, giving an aspect ratio $s/c = 1$. During molding, a rigid axis is inserted inside the plate at the leading edge; this axis has some roughness to prevent the rotation of the plate around it. This set-up reduces the flexible length of the chord to about 0.115 m. The plate is then immersed in a uniform flow, of velocity $U$, of a free surface water channel. The test section is 0.38 m wide, with a depth of water at rest of 0.45 m.

As shown in Fig. 1(a), the axis is attached to an inverted U-frame such that the plate, at the leading edge, is maintained parallel to channel flow. This inverted U-frame is set into vertical motion by a computer-controlled linear actuator, which allows to impose an arbitrary heave motion to the leading edge. In the present experiments, the leading edge has been forced into a harmonic heave motion: $A_{LE}\cos(2\pi ft)$. The plate is confined between two vertical walls separated from the plate by less than 1 mm. The role of these confinement walls is, first, to minimize the flow around the side edges of the plate and, second, the inverted U-frame being outside of these walls, to avoid the perturbations from the wake of the frame. In addition, free surface effects have been prevented by a rigid horizontal wall placed above the experiment. Channel and confinement walls have been made of transparent material to facilitate visualizations.

To investigate the response of the plate when forced into heave motion, visualizations have been carried out through the side wall of the water channel and recorded with a video camera. The successive shapes and positions of the plate centerline have then been extracted by image analysis of the recordings. A quantitative characterization of the plate response is achieved by measuring the simultaneous displacements of the leading and trailing edges as a function of time by means of two high-accuracy laser sensors (Fig. 1(a)).

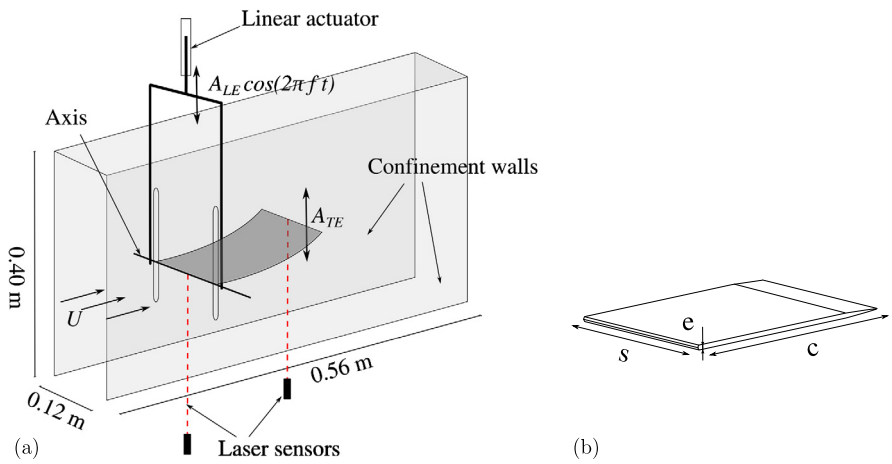


**Fig. 1.** Sketch of the experimental set-up (a) and of the flexible plate (b).

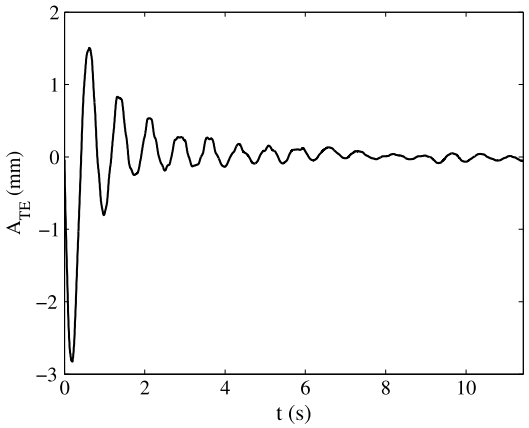


**Fig. 2.** Response of a plate to an impulse perturbation. The deflection of the trailing edge is plotted as function of time for the plate of bending rigidity $B = 0.053$ N m in water at rest.

In the present study, the variations of four experimental parameters have been considered. First, the frequency $f$ and amplitude $A_{\mathrm{LE}}$ of the forcing have been varied in the ranges $f = 0.2$–$8$ Hz and $A_{\mathrm{LE}} = 0.004$–$0.014$ m. Then, the flow velocity has been increased up to $U = 0.1$ m s$^{-1}$. This velocity is expressed in dimensionless form using the Reynolds number based on the chord: $Re = Uc/\nu$, where $\nu$ is the kinematic viscosity of water. Finally, three plate rigidities have been tested using different materials: $B = 0.018$, $0.028$, $0.053$ N m. For these three plates, the density relative to the water is about 1.2.

A typical experiment consists, for a plate of given bending rigidity, in fixing the Reynolds number $Re$ and the forcing amplitude $A_{\mathrm{LE}}$ and in recording the plate response as the forcing frequency $f$ is gradually varied. Experiments have been repeated changing $A_{\mathrm{LE}}$, $Re$, and using plates of different bending rigidity.

## 3. Results

Prior to the experiments with forcing, we have considered the response of the plate to an impulse perturbation of its trailing edge, in water at rest. The damped response to such a perturbation is shown in Fig. 2 for the plate of bending rigidity $B = 0.053$ N m. From this signal, we deduce the lowest natural frequency $f_0$ of the plate in water that will serve as a reference frequency in the following. For the three plates tested in the present study, we find the natural frequencies $f_0 =$ 0.75, 0.99, 1.30 Hz for bending rigidities $B = 0.018$, $0.028$, $0.053$ N m, respectively. Note that the ratios of these frequencies scale like the square root of the bending rigidity ratios (as expected from the vibration analysis of a cantilever beam) with an agreement better than 6%.

The response of the flexible plates to the harmonic forcing, $A_{\mathrm{LE}}\cos(2\pi f t)$, imposed at their leading edge is then considered. We first note that for all the cases tested the plate deforms mainly along the chord and its displacement is harmonic with the same frequency as the forcing. The displacement of the trailing edge can thus be expressed as $A_{\mathrm{TE}}\cos(2\pi f t + \phi)$ where $\phi$ is the phase relative to the leading edge displacement.

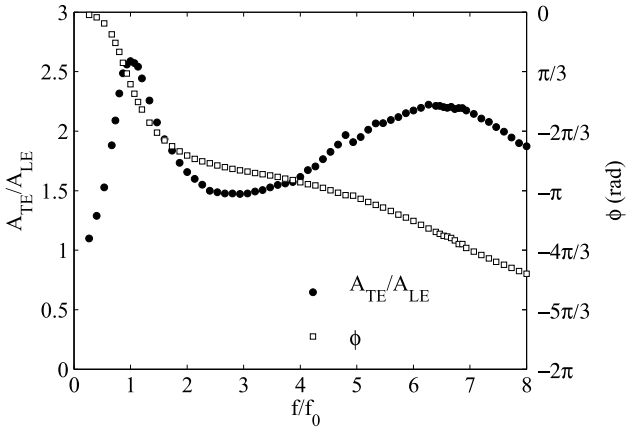


**Fig. 3.** Response of the plate to a harmonic heave forcing. The relative amplitude of the trailing edge displacement, $A_{TE}/A_{LE}$, and the corresponding phase shift $\phi$ are plotted as a function of the normalized forcing frequency $f/f_0$, for $A_{LE} = 0.004$ m, $Re = 6000$ and $B = 0.018$ N m.

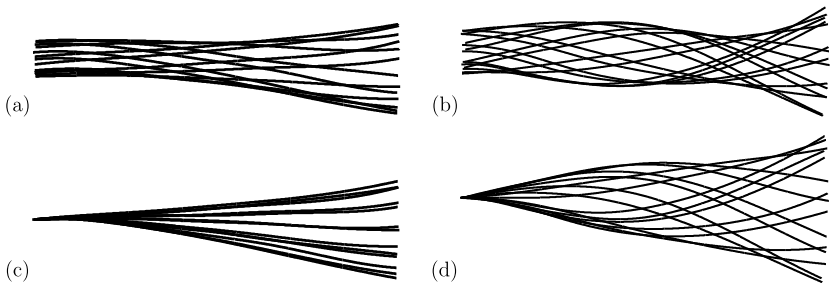


**Fig. 4.** Mode shapes, at the first $f/f_0 = 1$ (a), (c), and second resonance peak, $f/f_0 = 6.3$ (b), (d). These deformations are shown in the laboratory frame (a), (b) and in the frame attached to the leading edge (c), (d), $A_{LE} = 0.004$ m, $Re = 6000$ (flow from left to right) and $B = 0.018$ N m.

The plate response is characterized by measuring the evolution of the relative amplitude $A_{TE}/A_{LE}$ and the phase $\phi$ as the forcing frequency $f$ is varied. This response is illustrated in Fig. 3 for a representative case: $A_{LE} = 0.004$ m, $Re = 6000$ and $B = 0.018$ N m. In this plot, $f$ is made dimensionless using the natural frequency $f_0$ of the plate.

Remarkably, the amplitude curve exhibits two distinct peaks. The first peak is sharp and occurs at a frequency $f$ close to the natural frequency $f_0$, with a maximum of the trailing edge amplitude more than 2.5 times the forcing amplitude. The second peak, at a frequency $f/f_0$ between 6.0 and 6.5, is flatter and lower in amplitude. It is recalled that the three first natural vibration modes of a clamped plate have dimensionless wavenumbers $k_0c = 1.875$, $k_1c = 4.694$, and $k_2c = 7.855$ and that the ratios of the corresponding natural frequencies $f_0$, $f_1$ and $f_2$ scale like the square of wavenumber ratios. It results that $f_1/f_0 = (k_1/k_0)^2 \approx 6.3$. We can thus conclude that the two peaks observed at $f \approx f_0$ and $f_1$ in Fig. 3 correspond to resonances of the forcing with the first two natural structural modes. According to this analysis the third resonance peak would be expected at a frequency $f \approx f_2$ with $f_2/f_0 = (k_2/k_0)^2 \approx 17.6$, which is outside of the frequency range explored in the present experiments.

The evolution of the trailing edge phase $\phi$ relative to the imposed leading edge motion is also shown in Fig. 3. The phase appears to be close to $-\pi$ far from the two resonance peaks and approaches $-\pi/2$ at the first peak which is what is expected from a simple damped oscillator model. In contrast, it is not possible to distinguish a clear trend for $\phi$ at the second peak, where it continuously varies between $-3$ and $-5$.

In Fig. 4, the deformation of the plate at the two resonant peaks is illustrated by plotting superimposed views of the plate centerline during one forcing cycle. It should be noted that direct visualizations of the plate do not reveal significative deformations along the span, such that the plate deflection is well represented by the centerline displacement. It can also be remarked that a weak up-and-down asymmetry in the mode shape is apparent, which is due to the plate material being slightly denser than water.

Figs. 4(a) and (b) show the mode shapes at the two resonance peaks $f/f_0 = 1$ and 6.3, respectively, in the laboratory frame. Contrary to the first mode, the second mode exhibits a neck close to its trailing edge showing that higher structural modes are involved at high frequencies. The same modes are represented in the frame attached to the plate leading edge in Figs. 4(c) and (d). These views reveal their close similarities with the flutter instability modes of a clamped plate immersed in a uniform flow investigated by Eloy et al. [24], among others. Note that these deformations are different from the natural modes of a flexible beam in vacuum. In particular, the second mode (Fig. 4(d)) does not exhibit a node but only a pseudo-node or neck, revealing once again that the structural modes and their corresponding frequencies correspond to

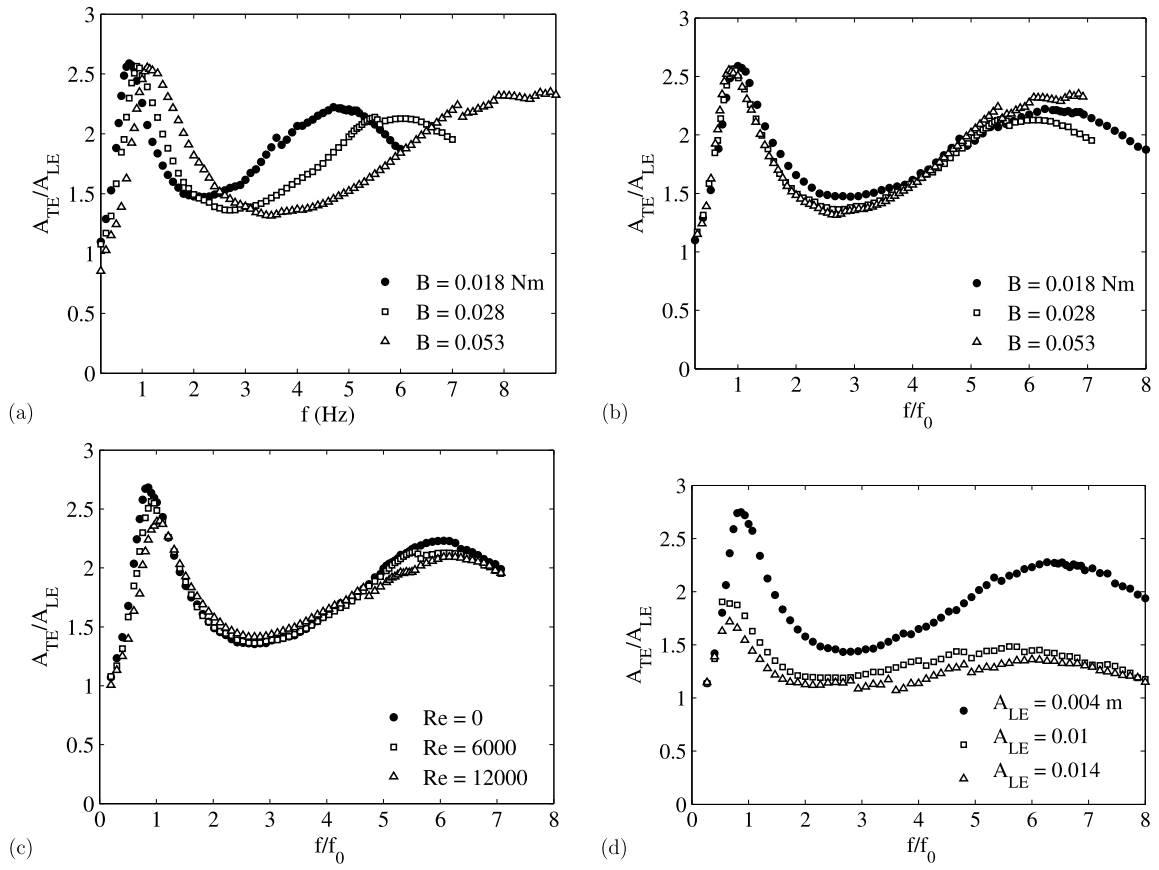


**Fig. 5.** Effects of the experimental parameters on the frequency response. Response curves as a function of the forcing frequency $f$ (a) and of the normalized frequency $f/f_0$ (b) for $A_{LE} = 0.004$ m, $Re = 6000$ and three values of the bending rigidity $B$. Frequency response for $A_{LE} = 0.004$ m, $B = 0.028$ N m and three values of the Reynolds number $Re$ (c) and for $Re = 6000$, $B = 0.018$ N m and three values of the forcing amplitude $A_{LE}$ (d).

the system plate + surrounding fluid and not the plate alone, as emphasized by Michelin and Llewellyn Smith [17] in their numerical study.

So far, we have described the frequency response of a flexible plate for fixed values of the forcing amplitude $A_{LE}$, the Reynolds number $Re$, and the bending rigidity $B$. We will examine now how variations of these parameters affect the frequency response. To do so, the same protocol is used: $A_{LE}$, $Re$ and $B$ are fixed and the relative response $A_{TE}/A_{LE}$ is plotted as function of the normalized frequency $f/f_0$ (Fig. 5).

### 3.1. Effect of the plate rigidity

In Fig. 5(a), the response curves are plotted as a function of the dimensional forcing frequency $f$ for three values of the plate rigidity $B$. We note that the amplitude maxima are not affected by changing $B$ and that the resonance peaks move toward higher frequency as $B$ is increased. However, the natural frequencies $f_0$ increasing with the plate rigidity, when the response curves are plotted using the dimensionless frequency $f/f_0$, they all collapse on a single curve as seen in Fig. 5(b). In conclusion, in the limit of the present study, which considers plates with bending rigidities varying by a factor 3, we could not detect any significant effect of the plate rigidity, as long as the frequency is properly normalized with the natural frequency $f_0$.

### 3.2. Effect of the Reynolds number

The effect of the Reynolds number $Re = Uc/\nu$ on the plate response is illustrated in Fig. 5(c) representing the frequency response for three values of $Re$. The first value is $Re = 0$ corresponding to water at rest, the two others are 6000 and 12,000, corresponding to $U = 0.05$ and $0.1$ m s$^{-1}$, respectively. We observe both a decrease of the amplitude maxima and a shift of the resonance peaks toward higher frequencies, as $Re$ is increased. This latter observation is due to the normalization performed using the natural frequency $f_0$ of the plate in water at rest while the natural vibration modes are modified by a surrounding flow as noted in [17]. However, these variations in the plate response as $Re$ is changed appear only minor. This is likely due to the large values of the reduced frequency $f_r = \pi f c/U$, which measures the ratio between the typical time

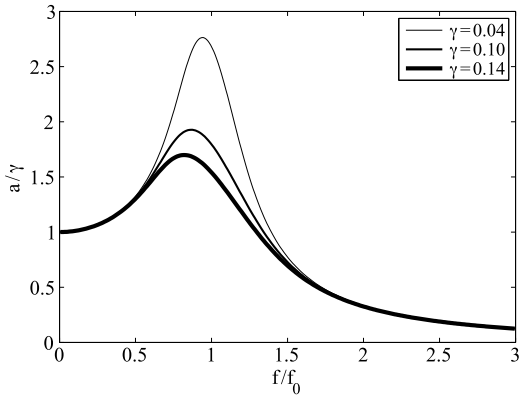


**Fig. 6.** Response curves obtained with Eq. (3) for different values of the forcing $\gamma$. The following parameters have been used: $f_0 = 1/2\pi$, $\mu = 0.1$, $\nu = 3$, and $\gamma = 0.04$, 0.1, or 0.14.

taken by a fluid particle to travel along the chord to the forcing period. For smaller values of $f_r$, one would expect the wake to become more important and to affect the frequency response more significantly.

### 3.3. Effect of the forcing amplitude

Contrary to the other parameters tested, variations of the forcing amplitude $A_{LE}$ have a strong influence on the plate response. This influence is shown in Fig. 5(d), where the frequency response is plotted for three values of $A_{LE}$. An increase of the forcing amplitude by a factor of 3.5 (from 0.004 to 0.014 m) leads to a decrease of the relative response amplitude of the trailing edge by more than 30% and a slight decrease of the normalized frequency at the resonance peaks. This important effect of the forcing amplitude is a signature of non-linear effects.

These non-linearities likely originate from the large-amplitude plate deformations, which introduce non-linear terms in both the plate and flow dynamical equations, through geometrical and damping terms. For instance, the impermeability condition, which ensures the coupling between the plate and the fluid, has to be applied on a displaced interface, yielding terms that depend non-linearly on the motion amplitude. These terms correspond to cubic non-linearities [25]. Another source of non-linearity is the drag force exerted on the plate normally to its surface as it moves, also called the resistive force, which corresponds to quadratic non-linearities [26].

Calling $x$ the amplitude of the first bending mode of the plate, we expect a weakly non-linear dynamical equation of the form

$$\ddot{x} + (2\pi f_0)^2 x + \mu\dot{x} + \nu|\dot{x}|\dot{x} + \delta x^3 = \gamma\cos(2\pi f t) \tag{1}$$

where the first two terms describe the bending mode of the plate as a harmonic oscillator (with eigenfrequency $f_0$), the third term is related to the internal damping of the plate ($\mu > 0$), the fourth term is the quadratic non-linearity due to the drag normal to the plate ($\nu > 0$), and the fifth term gathers all the cubic non-linearities originating from the fluid–structure interaction, the plate dynamics, and the fluid load (in reality there should also be terms of the form $x^2\ddot{x}$ and $x\dot{x}^2$). The right-hand side corresponds to the forcing due to the heaving motion, where $\gamma > 0$ without loss of generality. This equation is the classic Duffing oscillator with an additional quadratic term, $\nu|\dot{x}|\dot{x}$. It is beyond the scope of the present paper to calculate the coefficients $\mu$, $\nu$, and $\delta$ appearing in this equation, however, it can be formally solved by assuming

$$x(t) = a\cos(2\pi f t + \phi) + \text{h.o.t.} \tag{2}$$

where h.o.t. stands for "higher-order terms" and refers here to higher harmonics that can be neglected near resonance. Neglecting also the cubic non-linearities for simplicity, the dynamical equation (1) can be projected onto the main harmonics to give an implicit equation for the amplitude $a$ of the bending mode oscillations:

$$(2\pi)^4\left(f_0^2 - f^2\right)^2 a^2 + (2\pi)^2\left(\mu f + \frac{16}{3}\nu f^2 a\right)^2 a^2 = \gamma^2 \tag{3}$$

Solving this implicit equation shows, in particular, that at the resonance (i.e. $f = f_0$), the relative amplitude $a/\gamma$ is a monotonic decreasing function of $\gamma$. This is conform to the experimental observations, where the relative amplitude $A_{TE}/A_{LE}$ is also a decreasing function of the forcing amplitude $A_{LE}$. In Fig. 6, the relative amplitudes $a/\gamma$ obtained with Eq. (3) for different values of the forcing parameter $\gamma$ are plotted as a function of the normalized forcing frequency $f/f_0$. It shows a good qualitative agreement with the experimental measurements reported in Fig. 5(d) near the first resonance. In particular, the value of the relative response at its maximum (around $f \approx f_0$) is decreasing when the forcing amplitude is increased. The shift of the response peak towards lower frequencies for large forcing amplitude is also reproduced. However, the

second peak observed in Fig. 5(d) around $f/f_0 \approx 6$ is not reproduced in the model (Fig. 6) since it only accounts for a single natural mode of vibration whereas the flexible plate has an infinite number of structural modes.

The experimental results presented in Fig. 5(d) and the above discussion on the Duffing equation show that an accurate description of the plate response at resonance must include non-linear effects. It is important to stress that these non-linear effects are relevant even if the relative amplitude of the deformation, $A_{TE}/c$, and the angle between the plate and the flow direction are both relatively small. Yet, these effects are usually neglected in the literature, probably because until now, to our knowledge, there has not been any systematic measurements of the response of a flexible plate when the forcing amplitude is varied (see, e.g., [21–23]).

## 4. Conclusion

In summary, experiments have been conducted to investigate the response of a flexible plate in a uniform flow, when its leading edge is forced into a harmonic heave motion. This study focused in particular on the influence of the different experimental parameters on the characteristics of the frequency response.

As observed in previous studies, the response curves, representing the relative response amplitude with respect to the forcing frequency, exhibit peaks of resonance for the natural modes of the plate in the fluid flow. The flow velocity and the plate bending rigidity have only minor effects on the response curves as long as the forcing frequency is properly normalized with the natural mode frequency. In contrast, the forcing amplitude strongly affects the plate response indicating the importance of non-linearities in this system.

The present experiments performed with an idealized geometry can help to gain insight into the physical mechanisms of thrust production by flapping flexible appendages. It is known from the seminal work of Lighthill [27] that the thrust scales as the square of the trailing edge deflection amplitude in the linear limit. This study shows that this amplitude can be maximized when the flapping frequency is close to the frequency of one of the natural modes. However, the non-linear effects probably affect Lighthill's scaling of thrust production for large amplitude, and there is likely an optimal amplitude at which propulsion efficiency is maximized. Moreover, the present experimental results show that if one wants to model the fluid–structure interactions of a flapping flexible plate in a uniform flow plate, non-linear effects have to be taken into account. Such a model is currently being developed and will be subject of a forthcoming work.

## References

[1] M.J. Lighthill, Mathematical Biofluiddynamics, Society for Industrial and Applied Mathematics, 1975.
[2] S. Childress, Mechanics of Swimming and Flying, Cambridge University Press, Cambridge, UK, 1981.
[3] M.J. Lighthill, Hydromechanics of aquatic animal propulsion, Annu. Rev. Fluid Mech. 1 (1969) 413–446.
[4] M. Sfakiotakis, D.M. Lane, J.B.C. Davies, Review of fish swimming modes for aquatic locomotion, IEEE J. Ocean. Eng. 24 (2) (1999) 237–252.
[5] M.S. Triantafyllou, G.S. Triantafyllou, D.K.P. Yue, Hydrodynamics of fishlike swimming, Annu. Rev. Fluid Mech. 32 (2000) 33–53.
[6] R. Bainbridge, Caudal fin and body movement in the propulsion of some fish, J. Exp. Biol. 40 (1963) 23–56.
[7] F.E. Fish, G.V. Lauder, Passive and active flow control by swimming fishes and mammals, Annu. Rev. Fluid Mech. 38 (2006) 194–224.
[8] M.J. Lighthill, Aquatic animal propulsion of high hydromechanical efficiency, J. Fluid Mech. 44 (1970) 265–301.
[9] T.Y. Wu, Hydromechanics of swimming propulsion, J. Fluid Mech. 46 (1971) 337–355.
[10] M.S. Triantafyllou, G.S. Triantafyllou, R. Gopalkrishnan, Wake mechanics of thrust generation in oscillating foils, Phys. Fluids A 3 (12) (1991) 2835–2837.
[11] J.M. Anderson, K. Streitlien, D.S. Barret, M.S. Triantafyllou, Oscillating foils of high propulsive efficiency, J. Fluid Mech. 360 (1998) 41–72.
[12] L. Schouveiler, F.S. Hover, M.S. Triantafyllou, Performance of flapping foil propulsion, J. Fluids Struct. 20 (2005) 949–959.
[13] J.H.J. Buchholz, A.J. Smits, The wake structure and thrust performance of a rigid low-aspect-ratio pitching panel, J. Fluid Mech. 603 (2008) 331–365.
[14] C. Eloy, Optimal Strouhal number for swimming animals, J. Fluids Struct. 30 (2012) 205–218.
[15] J. Katz, D. Weihs, Hydrodynamics propulsion by large amplitude oscillation of an airfoil with chordwise flexibility, J. Fluid Mech. 88 (3) (1978) 485–497.
[16] S. Alben, Optimal flexibility of a flapping appendage in an inviscid fluid, J. Fluid Mech. 614 (2008) 355–380.
[17] S. Michelin, S.G. Llewellyn Smith, Resonance and propulsion performance of a heaving wing, Phys. Fluids 21 (7) (2009) 071902.
[18] P. Prempraneerach, F.S. Hover, M.S. Triantafyllou, The effect of chordwise flexibility on the thrust and efficiency of a flapping foil, in: Proc. 13th Int. Symp. on Unmanned Untethered Submersible Technology, 2003.
[19] S. Heathcote, I. Gursul, Flexible flapping airfoil propulsion at low Reynolds number, AIAA J. 45 (5) (2007) 1066–1079.
[20] C. Marais, B. Thiria, J.E. Wesfreid, R. Godoy-Diana, Stabilizing effect of flexibility in the wake of a flapping foil, J. Fluid Mech. 710 (2012) 659–669.
[21] P.A. Dewey, B.M. Boschitsch, K.W. Moored, H.A. Stone, A.J. Smits, Scaling laws for the thrust production of flexible pitching panels, J. Fluid Mech. 732 (2013) 29–46.
[22] S. Alben, C. Witt, T.V. Baker, E. Anderson, G.V. Lauder, Dynamics of freely swimming flexible foils, Phys. Fluids 24 (2012) 051901.
[23] D.B. Quinn, G.V. Lauder, A.J. Smits, Scaling the propulsive performance of heaving flexible panels, J. Fluid Mech. 738 (2013) 250–267.
[24] C. Eloy, R. Lagrange, C. Souilliez, L. Schouveiler, Aeroelastic instability of cantilevered flexible plates in uniform flow, J. Fluid Mech. 611 (2008) 97–106.
[25] C. Eloy, N. Kofman, L. Schouveiler, The origin of hysteresis in the flag instability, J. Fluid Mech. 691 (2012) 583–593.
[26] S. Ramananarivo, R. Godoy-Diana, B. Thiria, Rather than resonance, flapping wing flyers may play on aerodynamics to improve performance, Proc. Natl. Acad. Sci. USA 108 (2011) 5964–5969.
[27] M.J. Lighthill, Note on the swimming of slender fish, J. Fluid Mech. 9 (1960) 305–317.